P1.8

Adapting the Micropulse Lidar for Use as a Reference for Cloud Measurement

Aaron J. Poyer
Science Applications International Corporation
Sterling, VA

Richard Lewis
National Weather Service
Sterling, VA

1. INTRODUCTION

The National Weather Service (NWS) and Federal Aviation Administration (FAA) and Department of Defense (DoD) jointly participate in a Product Improvement (PI) Program to improve the capabilities of the Automated Surface Observing Systems (ASOS). ASOS has been in existence for almost 20 years and is currently the primary observing system at over 1000 airports and other observing sites nationwide.

The greatest challenge in the ASOS was to automate the visual elements of the observation; sky conditions, visibility and type of weather. An early limitation of ASOS was that the range of the ceilometer was limited to 4000 meters. This was primarily due to eye safety concerns associated with high power lasers and limitations in signal processing for detection of the weak returned laser signal from low power, eye-safe pulsed diode lasers (Imbembo, 1983 and Eberhard, 1986). With improvements in laser detector signal processing has come steady improvement in laser ceilometer range which now extends to 8000 meters and beyond.

2. DEFINITION OF SKY CONDITIONS

The National Weather Service Federal Meteorological Handbook No. 1 (FMH) (NOAA, 1996) defines sky condition as:

> "A description of the sky from the surface of the earth. For height … a ceilometer … or observer experience shall be used".

To do this the observer is given additional guidelines to code a surface aviation observation (METAR) to assist pilots and air traffic controllers in the safe control of aircraft. While there is necessarily some subjectivity in this definition, the goal is to provide information to pilots on conditions that will affect take-off, landing, or in flight operations. With the introduction of inexpensive LiDAR ceilometers and computer processing, it was possible to automate sky cover observations using sophisticated hierarchical clustering techniques. These techniques were introduced into NWS observing programs in 1975 and refined and enhanced before the wide scale deployment of ASOS in the 1990s (NOAA, 1985 and NOAA 1998).

* *Corresponding author address*: Aaron Poyer, Science Applications International Corporation, Sterling, VA 20166 aaron.poyer@ noaa.gov

3. ASOS CEILOMETER

The current ASOS ceilometer, the CT-12K shown in Figure 1, measures clouds to 4000 meters. ASOS algorithms can provide the height of clouds or obscurations aloft as well as an estimate of sky cover based on the "hit" percentages of the identified layers. Any clouds beyond this height must be augmented by observers using FMH procedures. These ceilometers are currently being replaced by a new ceilometer, the CL31 shown in figure 2, that will measure clouds to 8000 meters (Ravila, 2004**).**

Figure 1. National Weather Service ceilometer model K220 (range 4000 meters)

Figure 2. National Weather Service ceilometer model CL31 (range 8000 meters)

4. MICROPULSE LIDAR (MPL)

The MPL-4B-527 Micropulse Lidar uses a single lens arrangement to detect cloud bases. The single lens is shared by both the transmitting and receiving units. The transmitter is a neodymium yttrium lithium fluoride (Nd:YLF) pulsed laser diode, operating at a wavelength of 527nm. The receiving unit is a 178mm diameter Maksutov Cassegrain telescope with a focal length of 2400mm which collects received energy to a Silicon Avalanche photodiode for photon counting. The sensor is installed in an environmentally controlled enclosure, Figure 3, containing the laser, the laser controller, and the data acquisition systems, Figure 4. A climate control system (HVAC) is mounted externally and connected by a duct to provide heating and cooling to maintain an operationally acceptable temperature range. The HVAC unit and electronically controlled Kapton® strip heaters, mounted to the interior of the window glass, are used to reduce fogging and moisture build-up on the glass. The ASOS PI team added an external blower to assist in clearing the window glass of dust, remnant precipitation, and other environmental debris. The MPL-4B-527 has an advertised maximum range of 60,000 meters.

The MPL can also be operated in two different polarization modes (Flynn, 2007). Adding an actively-controlled liquid crystal retarder provides the capability to identify depolarizing particles by alternately transmitting linearly and circularly polarized light. This represents a departure from established techniques, which transmit exclusively linear polarization or exclusively circular polarization. Polarization-sensitive detection of elastic backscattered light is useful for detection of cloud phase and depolarizing aerosols. The implementation of this capability provides greater insight into the nature of the cloud or obscuring phenomena (liquid or crystal phase) and the presence of depolarizing aerosols.

Figure 3. Micropulse Lidar with blower and air conditioner

Figure 4. Micropulse Lidar inside conditioned housing

5. OBSERVER VS. CEILOMETER SKY CONDITIONS

The obvious requirements for a reference sensor for sky condition measurements are contained in the definitions cited in section 2. If an observer looking overhead can see a cloud or obscuring phenomenon, the reference sensor should be able to detect it. A cloud or obscuring phenomena is always associated with lowering visibility at the base of the layer. An observer sees contrast associated with the lowering of horizontal visibility of thick clouds and there will be agreement among observers that a cloud exist. As the clouds thin or transition to an elevated aerosol layer, there will be some differences between observers as to whether to report that layer. Similarly widespread thin cirrus with blue sky visible may be reported as an overcast layer by one observer and as a broken or even scattered layer by another. And at night, typically, a thin water droplet or ice crystal layer with stars visible will go unreported by the observer unless there is some indication by the ceilometer that a layer exists.

6. MICROPULSE LIDAR CLOUD HEIGHT

The basic techniques for deriving a vertical profile of extinction coefficient from the backscatter intensity received by a Lidar is discussed by Gaumet (1998). The backscatter power $P(Z)$ reaching the receiver is given by the following Lidar equation:

$$P(Z) = \frac{K_0 \beta(Z) \exp\left[-2\int_0^Z \alpha(z)dz\right]}{Z^2}$$

where K_0 is the apparatus constant, $\alpha(Z)$ the attenuation (or extinction) coefficient characterizing the optical path between cloud and ground (m^{-1}), and $\beta(Z)$ the backscatter coefficient characterizing the aerosol or cloud droplet density (m^{-1} sr^{-1}) at height Z.

This equation indicates that in a homogeneous atmosphere, $P(Z)Z^2$ decreases with height as an exponential function. In the presence of a cloud layer, the signal level undergoes a rapid increase because of enhanced backscattering of cloud droplets, then reaches its maximum value before decreasing to the level of backscatter from ambient air or disappearing into the background noise.

To invert the Lidar equation (1), another relationship between the two unknowns $\beta(Z)$ and $\alpha(Z)$ is needed. These two coefficients are dependent on the nature of the scattering particles and are related according to a power-law relationship of the form $\beta = k\alpha^n$, where k and n depend on the wavelength and size distribution of particles. For water clouds, $n \sim 1$ and $k \sim 0.05$ sr^{-1} and are assumed constant over the optical path. The Klett inversion (Klett, 1985) provides the stable solution:

$$\alpha(Z) = \frac{P(Z)Z^2}{\frac{P(Z_m)Z_m^2}{\alpha_m} + 2\int_Z^{Z_m} P(z)z^2\,dz}$$

The boundary value α_m is chosen at the far end Z_m of the height interval, near the maximum height level at which a usable signal is available and at a point allowing a reasonable estimate of α_m, defined as $\alpha_m = \alpha(Z_m)$. This value is generally more difficult to obtain here than near the ground at Z_0. The value of 10^{-4} m^{-1} was chosen for the extinction boundary value. The extinction coefficient profile can be converted to a profile of horizontal visibility by the equation for Meteorological Optical Range (Sheppard, 1983) :

$$V(Z) = \frac{\alpha(Z)}{3}$$

As an example, the MPL raw backscatter cloud profile for the cumulus cloud shown in Figure 5 is shown in Figure 6.

Figure 5. Cumulus clouds over the MPL

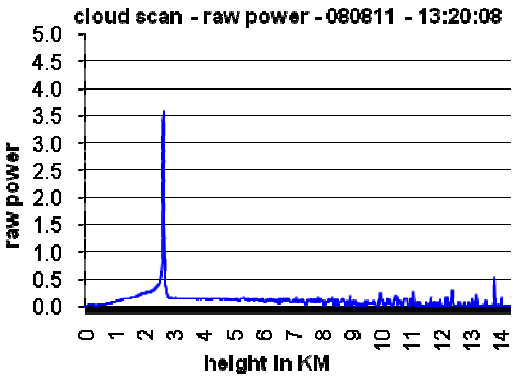

Figure 6. Micropulse Lidar backscatter signal

The raw profile can then be background adjusted and range normalized to obtain the $P(Z)Z^2$ profile and compute the visibility profile as shown in Figure 7.

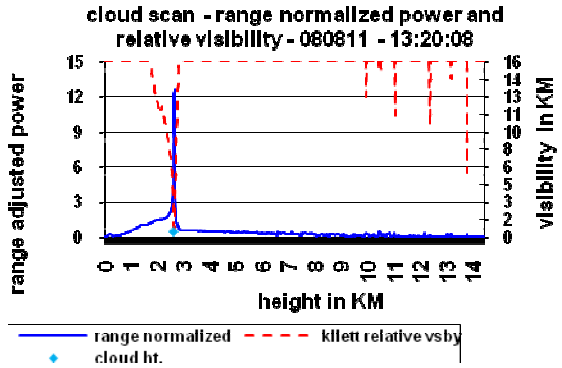

Figure 7. Micropulse Lidar background adjusted and range normalized backscatter signal for raw signal in figure 5. Visibility from Klett solution.

An example of thin cirrus overcast is shown in Figure 8. The raw return is shown in Figure 9. The primary difference between these thin ice crystal clouds and dense water droplet clouds is the deep layer of atmosphere from which returns are being received. This is seen in Figure 9 where the plot shows returns above noise between 10 and 11 kilometers.

Figure 8. Thin cirrus and contrails

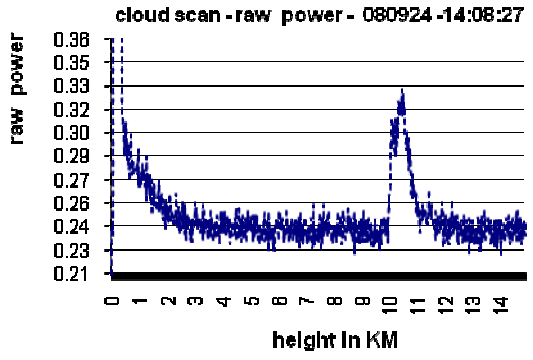

Figure 9. Micropulse Lidar backscatter signal for cirrus cloud.

The background adjusted and range normalized signal and Klett derived visibility is shown in Figure 10. In this figure, the drop in visibility is not as great and extends over a deep layer of atmosphere reflecting the signal seen in the raw graph.

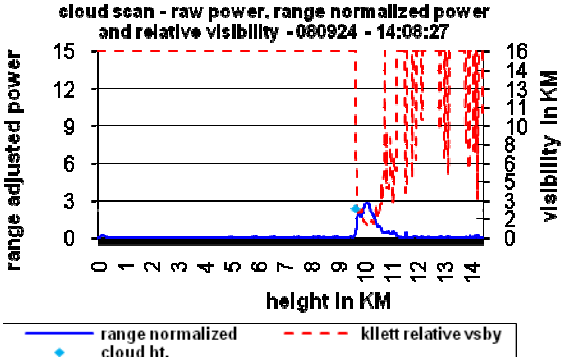

Figure 10. Micropulse Lidar background adjusted and range normalized backscatter signal for raw signal in figure 8. Visibility from Klett solution.

7. MPL CLOUD DETECTION ALGORITHM

The detection of clouds by the methodology presented in Section 6 is apparent. The cloud will exist where there is a rapid lowering of visibility entering the base of the cloud. An algorithm to detect these dense cloud bases is as follows:

$$\text{If } V_z < V_{cld} \text{ and } (V_{z+1} - V_{z-1}) > \Delta V_{cld} \text{ then } Z = Z_{cld}$$

Where V_z is the visibility at height Z. V_{cld} is the visibility at the cloud base and ΔV_{cld} is the change in visibility at the cloud base. Then Z_{cld} is the height of the cloud base. V_{cld} and ΔV_{cld} are empirically derived based on observer confirmation of the presence of a cloud base. The criteria are different for water droplet clouds with dense bases and thin water droplet or ice crystal clouds with thin diffuse bases.

In addition, for the case of thin clouds which do not meet the criteria in equation (4) but are deep enough to be visible to a surface based observer, the cloud base will be defined as the height at which the visibility begins to drop and remains below an average threshold visibility V_{av} for at least 300 meters or 20 of the MPL's atmospheric bins which are 15 meters wide:

$$\text{If } \frac{\sum_{n}^{n+20} V_n}{20} < V_{av} \text{ Then } Z_n = Z_{cld}$$

Where n is the bin number and Z_n is the height of bin n. Z_{cld} is then the height where the average visibility over 20 subsequent contiguous bins is less than V_{av}.

8. RESULTS

The MPL was operated at the NWS Sterling test facility from early April to September of 2008. During that period, observers took detailed cloud observations at least once per hour during daylight hours. This provided an extensive data set for comparing the MPL cloud detection algorithm with simultaneous human sky cover percentage estimates. These conditions were predominantly cumulus, stratocumulus, altocumulus, altostratus, and cirrus that are typical in mid latitudes through spring and summer. Based on these comparisons, the following values were derived for the visibility thresholds defined in equations (4) and (5):

For the case of dense water droplet clouds:

$V_{cld} = 0.64\ \text{km}$ and $\Delta V_{cld} = 0.064\ \text{km}$

For the case of thin water droplet and/ or ice crystal clouds:

$V_{cld} = 3.2\ \text{km}$ and $\Delta V_{cld} = 0.4\ \text{km}$ or $V_{av} = 4.8\ \text{km}$

The results for the cases shown in figures 7 and 10 are shown as cyan diamonds at the height where the cloud would be reported by the algorithm. Some additional examples of results of the algorithm compared to the CL31 and CT-12K are shown in figures 11 through 16. Obviously the CT-12K is range limited to 4 kilometers and the CL31 is range limited to 8 kilometers, which will lower their measured percentage compared to the MPL which can measure beyond 16 kilometers. However, in the first case the clouds were below 4 kilometers, the second case below 3 kilometers, and the third case the clouds were predominantly below 8 kilometers.

The first of the two graphs show the simultaneous hits from a CL31, CT-12K and MPL using the Klett algorithm and visibility criteria. The second graph shows the percentage of hits in the last 30 minutes from each system. Also shown on this graph is the observer estimated percentage of sky cover on the hour. The observer estimate is an instantaneous estimate based on sky cover over the ceilometers at the time of the observation. This would not be expected to be identical to the 30 minute average of cloud hits, but does provide an approximation of sky cover compared to the automated estimate.

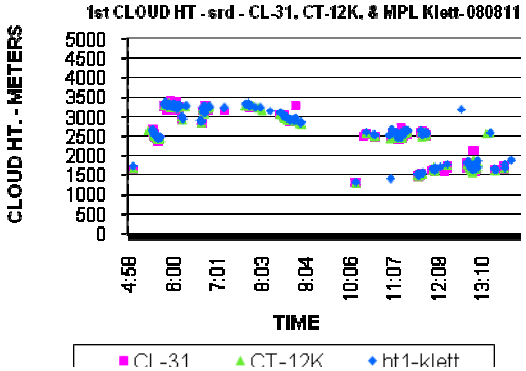

Figure 11. Cloud heights from CL31, CT-12K, and MPL Klett from 0500 to 1400 on 08/11/08

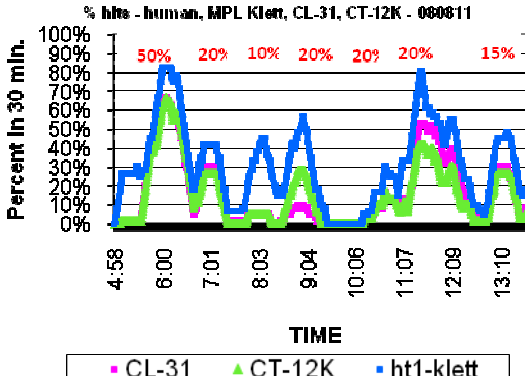

Figure 12. 30-minute cloud hit percentage for CL31, CT-12K, and MPL Klett for case in figure 10.

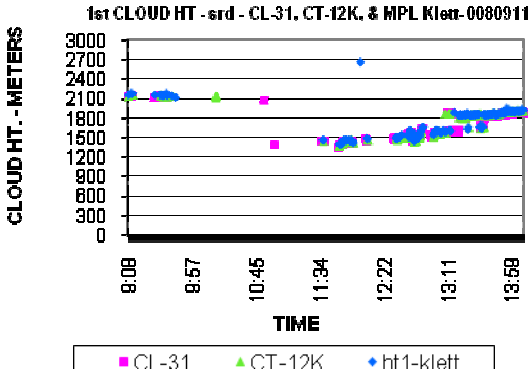

Figure 13. Cloud heights from CL31, CT-12K, and MPL Klett from 0900 to 1400 on 09/10/08

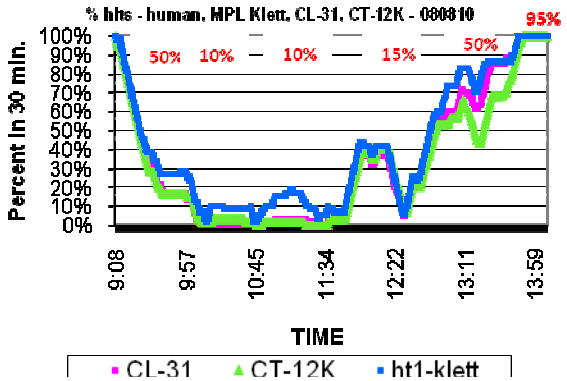

Figure 14. 30-minute cloud hit percentage for CL31, CT-12K, and MPL Klett for case in figure 12.

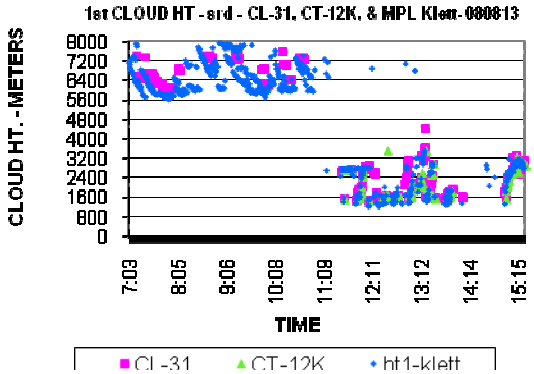

Figure 15. Cloud heights from CL31, CT-12K, and MPL Klett from 0700 to 1500 on 08/13/08

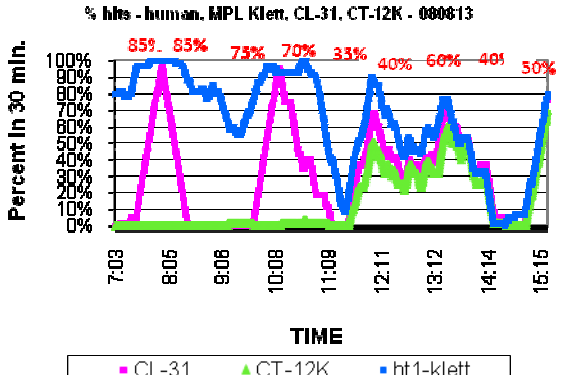

Figure 16. 30-minute cloud hit percentage for CL31, CT-12K, and MPL Klett for case in figure 14.

The cases shown above demonstrate that the MPL, with the larger optics and greater range will detect more clouds than either the current or replacement ASOS ceilometers. While the cloud conditions included in the analysis are extensive, it does not include any obvious cases of subvisible ice crystal clouds as described by Sassen (1989) or elevated smoke layers that might present special problems for the algorithm as described in section 7.

9. CONCLUSIONS

The MPL has been evaluated for use as a tool in determining cloud base for use as a reference in the evaluation of other commercial ceilometers. With the completion of MPL testing, the results demonstrate the capability of the MPL to accurately identify a cloud based on visibility changes associated with the cloud droplet or ice crystal attenuation. The backscatter associated with elevated aerosols trapped under inversions is distinguished from the cloud base by a simple algorithm that uses the visibility and rate of change in visibility at the cloud base. The method has been applied to liquid and ice crystal clouds. The use of two polarization modes also provides additional information about the nature of the cloud base. While there are some differences in the processing of the raw data and cloud detection algorithm, in general, both modes have proved effective in identifying clouds that are visible to surface based observers. Additional experience needs to be gained with elevated aerosol layers, e.g. smoke aloft, to determine if the algorithm can successfully identify those that are visible to surface based observers. Additionally a long standing concern with operational ASOS ceilometers is the reporting of subvisual ice crystal cloud layers as visible clouds. It is anticipated that the MPL will be a useful tool in increasing our understanding of these clouds and developing techniques to differentiate them from visible clouds.

ACKNOWLEDGMENTS

The authors would like to thank the staff at Sigma Space Inc. for support in installing and maintaining the MPL with special thanks to Savyasachee Mathur for his assistance throughout our test program. We would also like to express appreciation to Science Applications International Corporation personnel Dave Eckberg, Paul Oosterhout, and Michael Baldwin for the installation and maintenance of the ceilometers and MPL. Also thanks to Jennifer Dover, Gregory Whitaker, Brian Rice, Ryan Brown, and Caroline Normile who were part of the observing team that took manual cloud observations that supported the evaluation.

REFERENCES

Eberhard, W. L., 1986: Cloud signals from lidar and rotating beam ceilometer compared with pilot ceiling. *J. Atmos. Oceanic Technol.,* **3,** 499–512.

Flynn, C.J., A. Mendoza, Y. Zheng, S. Mathur, 2007: Novel polarization-sensitive micropulse lidar measurement technique, Opt. Express **15**, 2785-2790 (2007).

Gaumet, J. L., J. C. Heinrich, M. Cluzeau, P. Pierrard,

and J. Prieur, 1998: Cloud-Base Height Measurements with a Single-Pulse Erbium-Glass Laser Ceilometer. *J. Atmos. Oceanic Technol.*, **13**, 620–629.

Imbembo, S. M., and R. Lewis, 1983: An assessment of current cloud height indicator technology. Fifth Symp. on Meteorological Observations and Instrumentation*,* 11-15 April 1983, Toronto, ON, Canada, Amer. Meteor. Soc., 92–99.

Klett, J. D., 1981: Stable analytical inversion solution for processing lidar returns. *Appl. Opt.,* **20,** 211–220., 1986: Extinction boundary value algorithms for lidar inversion. *Appl. Opt.,* **25,** 2462–2464.

NOAA, National Weather Service, 1996: National Weather Service Handbook No. 7, Surface Weather Observations and Reports; U.S. DOC, Washington, DC, 405pp.

NOAA, National Weather Service, 1998: Automated Surface Observing System (ASOS) Users Guide, U.S.. Dept. of Commerce, Washington, DC, 61pp.

NOAA, National Weather Service, 1985:, "The Development of Reporting Algorithms for Automated Surface Observations", Test and Evaluation Division Report No. 1-85, Sterling, VA 29pp

Poyer, A.J., 2008: Evaluation of an MPL cloud detection algorithm. Symposium on Recent Developments in Applications of Radar and Lidar, 20-24 January, 2008, New Orleans, LA, P2.5

Ravila, P. and J. Räsänen, 2004: New ceilometer using enhanced single lens optics. Eighth Symposium on Integrated Observing and Assimilation Systems for Atmosphere, Oceans, and, and Land Surface, 12-15 January, 2004,Seattle, WA, P2.5

Sassen, M.K. Griffin, G.C. Dodd, 1989: Optical scattering and microphysical properties of subvisual cirrus clouds and climatic implications. *J. Appl. Meteor.,***28,** 91–98.

Sheppard, B.E., 1983: Adaptation to MOR. Fifth Symposium on Meteorological Observations and Instrumentation, 11-15 April, 1983, Toronto, Ont., Canada, P15.5